AECL-9500

ATOMIC ENERGY OF CANADA LIMITED

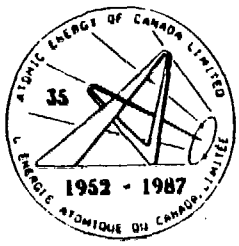

L'ÉNERGIE ATOMIQUE DU CANADA LIMITÉE

CHEMICAL DENITRATION OF AQUEOUS NITRATE SOLUTIONS

DÉNITRATION CHIMIQUE DES SOLUTIONS AQUEUSES DE NITRATE

K.A. BURRILL

Chalk River Nuclear Laboratories

Laboratoires nucléaires de Chalk River

Chalk River, Ontario

November 1987 novembre

ATOMIC ENERGY OF CANADA LIMITED

CHEMICAL DENITRATION OF AQUEOUS NITRATE SOLUTIONS

by

K.A. Burrill

Physical Chemistry Branch
Chalk River Nuclear Laboratories
CHALK RIVER, Ontario, K0J 1J0
1987 November

AECL-9500

L'ÉNERGIE ATOMIQUE DU CANADA, LIMITÉE

DÉNITRATION CHIMIQUE DES SOLUTIONS AQUEUSES DE NITRATE

par

K.A. Burrill

RÉSUMÉ

L'Installation pour Déchets Liquides Radioactifs (IDLR) (PAWL) des LNCR immobilisera dans le verre les produits de fission des déchets provenant de la production du Mo-99. On peut détruire les ions de nitrate par chauffage et aussi par réaction chimique avec l'acide formique (HCOOH). Etant donné que la dénitration chimique présente plusieurs avantages sur la dénitration thermique, on l'a étudié au cours de la mise au point du procédé de vitrification.

On examine, dans ce cas, les mécanismes à radicaux libres pour expliquer les données cinétiques sur la dénitration chimique des solutions d'acide nitrique avec l'acide formique. Un mécanisme est applicable à ≥ 1 mol/L HNO_3 et met en jeu le radical formiate ($HCOO\cdot$). L'autre mécanisme convient à ≤ 1 mol/L HNO_3, et met en jeu le radical hyponitreux ($HNO\cdot$). On a rédigé les bilans-masse de diverses espèces d'après la loi d'action de masse appliquée aux équations décrivant le mécanisme de réaction. On a obtenu des solutions analytiques et numériques qu'on a comparées.

On s'est servi de données bibliographiques sur la dénitration en lots pour déterminer certaines des constantes de vitesse de réaction tandis qu'on a déterminé les autres arbitrairement. On prédit avec précision la stoechiométrie et les tendances de concentrations de réactif observées pour des données sur la dénitration en lots. Il n'existe aucunes données bibliographiques à comparer avec les données prédites de temps d'induction négligeable.

Physico-chimie
Laboratoires Nucléaires de Chalk River
Chalk River, Ontario K0J 1J0
1987 novembre

AECL-9500

ATOMIC ENERGY OF CANADA LIMITED

CHEMICAL DENITRATION OF AQUEOUS NITRATE SOLUTIONS

by

K.A. Burrill

SUMMARY

The Plant for Active Waste Liquids (PAWL) at CRNL will immobilize in glass the fission products in waste from Mo-99 production. The nitrate ions in the waste can be destroyed by heating, but also by chemical reaction with formic acid (HCOOH). Since chemical denitration has several advantages over thermal denitration, it was studied in the course of vitrification process development.

Two free radical mechanisms are examined here to explain kinetic data on chemical denitration of nitric acid solutions with formic acid. One mechanism is applicable at > 1 mol/L HNO_3 and involves the formate radical ($HCOO^{\bullet}$). The second mechanism holds at < 1 mol/L HNO_3 and involves the hyponitrous radical ($HNO^{\bullet}$). Mass balances for various species were written based on the law of mass action applied to the equations describing the reaction mechanism. Analytical and numerical solutions were obtained and compared.

Literature data on batch denitration were used to determine some of the rate constants while others were set arbitrarily. Observed stoichiometry and trends in reactant concentrations are predicted accurately for batch data. There are no literature data to compare with the prediction of negligible induction time.

Physical Chemistry Branch
Chalk River Nuclear Laboratories
Chalk River, Ontario, K0J 1J0
1987 November

AECL-9500

TABLE OF CONTENTS

1. INTRODUCTION

A nitric acid solution of uranium, aluminum and fission products is accumulating in the Fissile Isotope Solution Storage Tank (FISST) as a result of Mo-99 production at CRNL. At the current production rate, FISST will be full in 1993 and will contain 24 000 L of high level liquid waste. The Plant for Active Waste Liquids (PAWL) is being built to recover the uranium from this solution and to immobilize the remaining waste in glass.

Calcining is a necessary step in any vitrification process. Calcining the precipitated nitrates at > 150°C destroys them and gives a rapid evolution of toxic NO_x which cannot easily be stopped or controlled once begun. Also, RuO_4 volatilizes during calcining and contaminates off-gas piping and eventually is flushed from the condenser by liquid evaporated from the glass melter. Lower waste acidity gives less RuO_4 and less volatilization during calcining.

Chemical denitration of liquid wastes by formic acid (HCOOH) was studied as a desirable step before calcining. Both simulated wastes and actual wastes were denitrated in laboratory scale equipment. The process was then demonstrated on the 5-inch diameter (12.5 cm) laboratory melter.

Two reaction mechanisms are examined here to explain the data. The hyponitrous acid radical cycle ($HNO^{\bullet}$) applies to < 1 mol/L NO_3^- and involves three reactions. The formate radical cycle ($HCOO^{\bullet}$) involves five reactions and applies to > 1 mol/L NO_3^-. Rate constants were estimated from the literature where possible, otherwise they were assigned values so that models of the mechanisms predicted the observed order-of-magnitude of nitrate ion concentration. Trends are predicted correctly by both models, as well as the stoichiometric ratio $HCOOH/HNO_3$ and off-gas composition (CO_2, NO_2, NO, N_2O) and their change with time.

2. LITERATURE REVIEW

One of the earliest denitration studies was by Longstaff and Singer (1). They studied HCOOH oxidation by nitrous acid (HNO_2) in nitric acid (HNO_3) at 25°C. Significant conclusions were that there was no reaction without HNO_2 and that HNO_3 does not participate in the rate-determining step, but it does oxidize reaction products. The following mechanism was proposed:

$$HCOOH + HNO_2 \rightarrow HCOO^{\bullet} + NO + H_2O \qquad (1)$$

$$HCOO^{\bullet} + HNO_2 \rightarrow CO_2 + NO + H_2O \qquad (2)$$

$$2NO + HNO_3 + H_2O \rightleftharpoons 3HNO_2 \qquad (3)$$

The rate-determining step is the bimolecular reaction in equation (1) for 0.1-2.5 $mol \cdot L^{-1}$ HNO_3.

Healy (2) noted that bubbling N_2 through a dilute HNO_3 solution removes HNO_2 and that the solution stays HNO_2 deficient in the dark. At low acidity,

1-4 mol•L^{-1} HNO_3, he proposed the following stoichiometry:

$$2HNO_3 + 3HCOOH \rightleftharpoons 2NO + 3CO_2 + 4H_2O \quad (4)$$

and at higher acidity

$$2HNO_3 + HCOOH \rightleftharpoons 2NO_2 + CO_2 + 2H_2O \quad (5)$$

The time for the reaction to start is called the induction time. Healy found that this was negligible at 100°C for > 2 mol•L^{-1} HNO_3.

Reaction kinetics were described empirically by

$$\frac{-dn}{d\theta} = k\,[HCOOH]^a\,[HNO_3]^3$$

where $k = 4.7 \times 10^{-4}\ L^{-2}\ mol^{-2} \cdot s^{-1}$
n = $[HNO_3]$
θ = time
a = reaction order with respect to HCOOH

The reaction mechanism was postulated to be:

Step one

$$2NO_2 + H_2O \rightleftharpoons HNO_2 + HNO_3 \quad (6)$$

Step two

$$HCOOH + HNO_2 \rightleftharpoons HC(=O)-O-NO + H_2O \rightleftharpoons HCOO\bullet + NO + H_2O \quad (7)$$

Clearly, if stripping NO_2 out of the solution with N_2 drives the HNO_2 concentration to low values the reaction with HCOOH will be imperceptible.

Saum, Ford and Platts (3) were concerned about Ru-106 volatilization during the calcination of fuel reprocessing waste. Low waste acidity lowers the RuO_4 concentration in the solution and should give low volatility. Chemical denitration with HCOOH was done on simulated wastes and the HCOOH and HNO_3 concentrations were followed with time. Batch experiments were done at 1-1.5 mol•L^{-1} HNO_3 concentrations; they show approximately exponential declines in reactant concentrations. At 1-1.5 mol•L^{-1} HNO_3, they find the kinetics in boiling waste solutions are described by:

$$\frac{-dn}{d\theta} = k_1\,[HCOOH]^{1.3}\,[HNO_3]^{1.4}$$

and at higher acidity

$$\frac{-dn}{d\theta} = k_2\,[HCOOH]^{1.5}\,[HNO_3]^{1.6}$$

with $k_1 = 3.7 \times 10^{-4}\ L^{1.7} \cdot mol^{-1.7} \cdot s^{-1}$

$k_2 = 5.9 \times 10^{-4}\ L^{2.1} \cdot mol^{-2.1} \cdot s^{-1}$

The reaction order with respect to HNO_3 is about one half that of Healy's.

Orebaugh (4) at Savannah River Laboratory studied denitration for similar reasons to Saum et al. Table 1, from his work, lists eleven possible reactions, most involving free radicals. He proposes the formate radical cycle at low HCOOH concentration and at high HNO_3 concentration;

$$HNO_3 + HCOO\bullet \rightarrow HNO_2 + CO_2 + OH\bullet$$

and $$HCOOH + OH\bullet \rightarrow HCOO\bullet + H_2O$$

Table 1 shows how HNO_2 produced from this cycle can be destroyed. These reactions give NO and NO_2 which are observed early in the reaction. At higher [HCOOH] and lower [HNO_3], he proposes the hyponitrous radical ($HNO\bullet$) cycle:

$$HNO_3 + HNO\bullet \rightarrow 2HNO_2$$

$$HNO_2 + HCOOH \rightarrow HNO\bullet + CO_2 + H_2O$$

Table 1 shows how reactions involving $HNO\bullet$ give N_2 and N_2O, seen toward the end of the reaction. Figure 1 from Orebaugh also shows how a simulated waste ($0.7\ mol \cdot L^{-1}\ HNO_3 + 0.35\ mol \cdot L^{-1}\ Fe(NO_3)_3 + 0.35\ mol \cdot L^{-1} Al(NO_3)_3 + 1.0\ mol \cdot L^{-1}\ NaNO_3$) is postulated to yield its NO_3^- for destruction: first the acid, then the iron, then the $Al(NO_3)_3$ in two parts, and finally, a fifth zone with $NaNO_3$ which he terms "unreactive".

Nakamura et al. (5) were able to denitrate simulated wastes completely, including $NaNO_3$, provided a Pt group element from fission was dissolved in the waste at a simulated waste concentration of $> 0.03\ mol \cdot L^{-1}$. Kubota et al. (6) used 0.1 L of $2\ mol \cdot L^{-1}\ HNO_3$ or simulated waste in a flask with a reflux condenser to study the effect of [NO_2^-] on the induction time. They found that:

(i) For $2\ mol \cdot L^{-1}\ HNO_3$, the induction time falls as the HCOOH addition rate rises.
(ii) The induction time falls from ~ 5 min for boiling $2\ mol \cdot L^{-1}$ HNO_3 to < 1 min for $0.05\ mol \cdot L^{-1}\ NaNO_2$ in the $2\ mol \cdot L^{-1}\ HNO_3$.
(iii) The HCOOH must be added within 2 min of adding $NaNO_2$ to the waste to get the benefit of reduced induction time. After 10 minutes of standing with $NaNO_2$, the benefit is lost.
(iv) The induction time falls as the HNO_3 concentration rises to an asymptotic value of ~ 2 min at $10\ mol \cdot L^{-1}\ HNO_3$.

German workers at Karlsruhe have also studied chemical denitration. In a move to reduce toxic NO_2 gas production, the waste is added to HCOOH so that the nitrate concentration is always very low (7). Holze et al. (8) indicate that reaction kinetics are described by

$$\frac{-dn}{d\theta} = k_o e^{-E_o/RT}[HCOOH]^2\ [HNO_3]^3$$

where

$$k_o = 1.45 \times 10^{16}\ L^4 \cdot mol^{-4} \cdot s^{-1}$$

$$E_o = 136\ kJ/mol$$

and the heat of reaction, ΔH, is given as -370 kJ/mol HNO_3 destroyed, for $[HNO_3] < 7\ mol \cdot L^{-1}$. The induction time τ is described by

$$\frac{1}{\tau} = k_o^1 e^{-E/RT}[HCOOH]^3\ [HNO_3]$$

Attention will now be focussed on Orebaugh's reaction mechanisms.

3. REACTION MECHANISMS

The literature review noted that nitrous acid (HNO_2) is the essential intermediate in the denitration reaction. Orebaugh's summary of possible reactions (2) is given in Table 1. He notes that:

(i) equilibrium for reaction (1) lies far to the left in highly acid solution so it does not supply much HNO_2.

(ii) from the observation that NO is not produced by denitration of highly acidic solution, reaction (2) is not prominent either.

(iii) two possible reactions to supply HNO_2 then remain; they are via the formate radical $HCOO^\cdot$ or the hyponitrous acid radical $HNO^\cdot$. Reactions are then:

$HNO_3 + HCOO^\cdot \longrightarrow HNO_2 + CO_2 + OH^\cdot$ (reaction 3)
$HCOOH + OH^\cdot \longrightarrow HCOO^\cdot + H_2O$ (reaction 3a), or,
$HNO_3 + HNO^\cdot \longrightarrow 2HNO_2$ (reaction 4)
$HNO_2 + HCOOH \longrightarrow HNO^\cdot + CO_2 + H_2O$ (reaction 5)

(iv) the hyponitrous acid radical cycle is probably important for HNO_2 production at low HNO_3 concentration. This happens near the end of a denitration, and the result will be N_2O production via reactions 9 and 10.

(v) at high acidity, HNO_2 is oxidized by HNO_3 to give NO_2 (reaction 6). Thus, less HNO_2 is available to react directly with HCOOH (reaction 5) to give $HNO^\cdot$, so little N_2O will be seen.

(vi) since there will be little $HNO^\cdot$ available for HNO_2 production at high acidity, then reactions 3, 3a involving $HCOO^\cdot$ and $OH^\cdot$ must dominate.

(vii) once the acidity falls and reaction 6 declines in rate, reactions 7 and 8 become noticeable and NO is seen.

The $HNO^\cdot$ radical cycle used here is then:

$HNO_2 + HCOOH \longrightarrow HNO^\cdot + CO_2 + H_2O$ (reaction 5)
$HNO_3 + HNO^\cdot \longrightarrow 2HNO_2$ (reaction 4)
$2HNO^\cdot \longrightarrow N_2O + H_2O$ (reaction 10)

Reactions 4, 5 and 10 show the classical initiation, propagation, and termination steps of a free radical chain.

The $HCOO^{\bullet}$ radical cycle used here is then:

$HNO_3 + HCOO^{\bullet} \longrightarrow HNO_2 + CO_2 + OH^{\bullet}$ (reaction 3)
$HCOOH + OH^{\bullet} \longrightarrow HCOO^{\bullet} + H_2O$ (reaction 3a)
$HNO_3 + HNO_2 \longrightarrow 2NO_2 + H_2O$ (reaction 6)
$HNO_2 + HCOOH \longrightarrow NO + HCOO^{\bullet} + H_2O$ (reaction 7)
$HNO_2 + HCOO^{\bullet} \longrightarrow NO + CO_2 + H_2O$ (reaction 8)

Again, the initiation, propagation, and termination steps are evident. Reaction 6 is a bimolecular reaction in parallel with the free radical reactions and it accounts for NO_2 production.

4. MATHEMATICAL MODELLING

In a batch reaction, the reactants are mixed at the beginning of the reaction and nothing more is added. In a semi-batch reaction, one of the reactants is added at a constant rate to the other. At some time into the reaction, the reactant feed is stopped, and the reaction proceeds as a batch reaction.

Each of the proposed mechanisms will be examined for the batch reaction condition. Then, the semi-batch condition will be considered.

4.1 Batch Conditions

4.1.1 $HNO^{\bullet}$ Radical Cycle

Single symbols will be used for simplicity to denote the various chemical species. These are:

$n = HNO_3$

$h = HNO_2$

$f = HCOOH$

$f^* = HCOO^{\bullet}$

$h^* = HNO^{\bullet}$

θ = time

The reactions may be rewritten with these symbols as:

$n + h^* \xrightarrow{k_4} 2h$ (reaction 4)

$h + f \xrightarrow{k_5} h^* + CO_2 + H_2O$ (reaction 5)

$2h^* \xrightarrow{k_{10}} N_2O + H_2O$ (reaction 10)

with the rate constants as shown. Mass balances for each species in a constant volume system are then:

$$\frac{dn}{d\theta} = - k_4 nh^* \qquad \ldots(1)$$

$$\frac{df}{d\theta} = - k_5 hf \qquad \ldots(2)$$

$$\frac{dh}{d\theta} = 2k_4 nh^* - k_5 hf \qquad \ldots(3)$$

$$\frac{dh^*}{d\theta} = k_5 hf - k_4 nh^* - k_{10}(h^*)^2 \qquad \ldots(4)$$

Typically, the free radical concentration is small and reaches steady-state quickly, so $\frac{dh^*}{d\theta} \approx 0$. A numerical solution of the above system of equations by FORSIM (9) showed that $\frac{dh}{d\theta} \approx 0$ was also a reasonable assumption. The rate constants used will be discussed later in this section.

To solve these equations, apply the above steady-state assumption to get:

$$2k_4 nh^* = k_5 hf \qquad \ldots(5)$$

and substituting for $k_5 hf$ in equation (4) gives:

$$h^* = \frac{k_4}{k_{10}} n \qquad \ldots(6)$$

Substituting for h^* in equation (1) gives:

$$\frac{dn}{d\theta} = \frac{k_4^2}{k_{10}} n^2$$

and integration with boundary condition $n = n_o$, $\theta = 0$ gives:

$$n = \frac{n_o}{1 + \frac{k_4^2}{k_{10}} n_o \theta} \qquad \ldots(7)$$

Substituting equation (6) into equation (5) gives:

$$h = \frac{2\, k_4^2}{k_5 k_{10}} \frac{n^2}{f} \qquad \ldots(8)$$

Finally, substituting for h, then n in equation (2) and integrating with $f = f_o$, $\theta = 0$ gives:

$$f = f_o - 2n_o + \frac{2n_o}{\left(1+\frac{k_4^2}{k_{10}} n_o\theta\right)} \qquad \ldots(9)$$

Substituting equation (5) into equation (1) shows that:

$$2\frac{dn}{d\theta} = \frac{df}{d\theta} \quad \text{or} \quad \frac{df}{dn} = 2$$

Thus, the stoichiometric ratio is two HCOOH molecules used for each HNO_3 molecule. This is predicted at low HNO_3 concentration. If $f_o > 2n_o$, equation (9) shows that f will go to some residual value and all the HNO_3 will be destroyed. If $f_o < 2n_o$, then the reaction will continue until all the HCOOH is used, and residual HNO_3 remains, called n_r. This value may be calculated simply from the stoichiometry as:

$$n_r = n_o - \frac{f_o}{2} \qquad \ldots(10)$$

Equations (7) and (10) may be combined to find the time θ_r, at which the reaction stops as:

$$\theta_r = \frac{k_{10}}{k_4^2}\left\{\frac{1}{n_r} - \frac{1}{n_o}\right\} \qquad \ldots(11)$$

Equation (9) will predict $f < 0$ beyond θ_r and clearly should not be applied beyond θ_r. Figures 2 and 3 show the relative change in HNO_3 and HCOOH concentrations versus time for various $\frac{f_o}{n_o}$ values in a batch reaction. While there are separate curves for [HCOOH] vs θ depending on f_o, there is only one curve for [HNO_3] vs θ up to the time when all the HCOOH has been consumed.

4.1.2 Batch Reaction Data

Saum, Ford, and Platts (3) did batch and semi-batch denitration with a simulated waste solution and formic acid. A refluxed system was apparently used, so the solution volume should have remained roughly constant. For 6 mol/L. HNO_3 in the waste, the HCOOH was added slowly over ~40 minutes. Waste volume in their experiments was not given but was probably < 1 L. For 1-1.5 mol/L. HNO_3, the waste and HCOOH were mixed batch-wise and samples were taken periodically to follow the HNO_3 and HCOOH concentrations. Data from these latter experiments are of most interest for modelling purposes because they do not introduce the added complexity of HCOOH addition rate when trying to get analytical solutions.

Figures 4 and 5 give Saum et al. batch data replotted as relative n and f concentrations. When compared with predictions from the HNO• radical model, the trends predicted by the model are correct, but the observed fine structure is different from the predictions. For example, the data show a limiting HNO_3 concentration being approached at $\frac{n}{n_o} = 0.5$ for $\frac{f_o}{n_o} = 1.5$, while the model predicts $\frac{n}{n_o} = 0.25$.

Figure 5 data show that there is still substantial HCOOH left in the solution to react at θ=100 min, but this has little effect on the residual HNO_3.

Figure 6 gives the observed reaction stoichiometry versus HNO_3 concentration for both batch and semi-batch experiments. At HNO_3 concentrations of 0-1 mol/L., the ratio is $\frac{df}{dn}=2$, in agreement with the HNO• radical model.

4.1.3 Formate Radical Cycle

The reactions already given may be rewritten as:

$n+f^* \xrightarrow{k_3} h + CO_2 + OH^*$ (reaction 3)

$f+OH^* \xrightarrow{k_{31}} f^*+H_2O$ (reaction 3a)

$n+h \xrightarrow{k_6} 2NO_2 + H_2O$ (reaction 6)

$h+f \xrightarrow{k_7} NO + f^* + H_2O$ (reaction 7)

$h+f^* \xrightarrow{k_8} NO + CO_2 + H_2O$ (reaction 8)

The steady-state assumption may be applied to the free radicals in this system. Mass balances for the two free radicals with $\frac{df^*}{d\theta} = \frac{dOH^*}{d\theta} \approx 0$ may be solved to yield

$$f^* = \frac{k_7 f}{k_8} \quad \text{and} \quad OH^* = \frac{k_3 k_7 n}{k_{31} k_8}$$

Mass balances for the remaining species in a constant volume system are then:

$$\frac{dn}{d\theta} = \frac{-k_3 k_7 nf}{k_8} - k_6 nh \qquad \ldots(12)$$

$$\frac{df}{d\theta} = \frac{-k_3 k_7 nf}{k_8} - k_7 nf \qquad \ldots(13)$$

$$\frac{dh}{d\theta} = \frac{k_3 k_7}{k_8} nf - 2\, k_7 hf - k_6 nh \qquad \ldots(14)$$

Applying the steady-state assumption to the intermediate h yields:

$$h = \frac{k_3 k_7 \quad nf}{k_8 \ (k_6 n + 2k_7 f)}$$

FORSIM solutions to equations (12) to (14) with reasonable values for rate constants show that $k_6 n \ll 2k_7 f$ for the best fit to the Saum et al. data, so that:

$$h = \frac{k_3 n}{2k_8} \qquad \ldots(15)$$

Substitute equation (15) into equations (12) and (13) with $\beta = \frac{k_8}{k_3}$ to get

$$\frac{dn}{d\theta} = - \frac{k_7 nf}{\beta} - \frac{k_6 n^2}{2\beta} \qquad \ldots(16)$$

$$\frac{df}{d\theta} = - \frac{3}{2} \frac{k_7 nf}{\beta} \qquad \ldots(17)$$

Dividing one equation by the other yields:

$$\frac{dn}{df} = \frac{2}{3} + \frac{k_6}{3k_7} \frac{n}{f} \qquad \ldots(18)$$

This equation shows that $\frac{df}{dn} < 1.5$, in agreement with the data in Figure 6 for intermediate HNO_3 concentrations. When $n = 0$, $\frac{df}{dn} = 1.5$ from equation (18) whereas the Figure 5 data indicate $\frac{df}{dn} = 2$. Clearly, the $HCOO^{\bullet}$ model does not apply here. Equation (18) may be integrated with $n = n_o$, $f = f_o$ to give:

$$n = \frac{2}{3} \frac{f}{(1-K)} + \left\{ n_o - \frac{2}{3} f_o \right\} \left\{ \frac{f}{f_o} \right\}^K \qquad \ldots(19)$$

where $K = \frac{k_6}{3k_7}$

Substitute equations (15) and (19) into (13) and solve for f to get:

$$f = \frac{\mu B}{(e^{B\theta} - \mu A)} \qquad \ldots(20)$$

where $\mu = \frac{f_o}{Af_o+B}$

$$A = \frac{k_7}{\beta(1-K)}$$

$$B = \frac{k_7}{2\beta}(3n_o - 2f_o)$$

and $\left\{\frac{f}{f_o}\right\}^K = 1$ was assumed

Figures 7 and 8 give predictions of equations (19) and (20) which may be compared with the Saum et al. data for a batch reaction with HCOOH. Rate constants used in the calculations are:

Rate Constants used in the HCOO• Cycle Model

rate constant	value (L/mol•min)
k_3	1×10^4
k_6	100
k_7	500
k_8	5×10^8

The derivation of these constants is discussed in Appendix 1.

Also given in Figures 7 and 8 are FORSIM solutions to equations (12), (13) and (14) with the same rate constants. The analytical and numerical solutions deviate when the HCOOH concentration approaches the HNO_3 concentration. This is probably due to the assumption of $k_6 n \ll 2k_7 f$ used in the derivation of equation (15). Free radical reactions like reactions (3) and (8) are expected to have larger rate constants than bimolecular reactions such as reactions (6) and (7).

4.1.4 Comparison of Both Models

The HNO• and HCOO• models predict the Saum et al. batch rate data on reactant concentrations equally well. However only the HNO• model predicts the correct stoichiometry seen in the batch reactions at $[HNO_3] \approx 1$ mol/L or less. At higher $[HNO_3]$, the stoichiometry $\frac{df}{dn} \approx 1.5$ applies up to 4 mol/L HNO_3 and the HCOO• model is thus recommended in the region 1-4 mol/L.

4.1.5 Induction Time

The time lag between mixing the reactants and the start of an observable reaction is called the induction time τ. The formate radical cycle model can be used to predict the functional dependence of this time. For a batch reaction, both HCOOH and HNO_3 are at maximum value at $\theta=0$, but HNO_2 is zero initially and must be produced by reaction.

From equation (14), the growth in HNO_2 may be approximated by:

$$\frac{dh}{d\theta} = \frac{k_3 k_7 n_o f_o}{k_8} \qquad \ldots(21)$$

If $h = h_c$ for a significant reaction rate, then $\theta = \tau$ and integration gives:

$$\tau = \frac{h_c}{\frac{k_3 k_7 n_o f_o}{k_8}} \qquad \ldots(22)$$

Thus, for a batch reaction, $\tau \alpha \frac{1}{n_o f_o}$

If equation (15) is used to describe h_c as:

$$h_c = \frac{k_3 n_o}{2k_8}$$

then:
$$\tau = \frac{1}{2k_7 f_o} \qquad \ldots(23)$$

Evaluation with $k_7 = 500$ L/mol·min and $f_o = 1$ mol/L gives

$\tau = 10^{-3}$ min = 0.06 s.

The HNO· radical cycle model can also be used to estimate τ. Production of HNO_2 and HNO· at small times may be estimated from equations (3) and (4) as:

$$\frac{dh}{d\theta} = 2k_4 n_o h^*$$

$$\frac{dh^*}{d\theta} = k_5 h f_o$$

These may be solved simultaneously with boundary conditions $h = h_o$, $\theta = 0$ and $h = h_c$ for $\theta = \tau$ to give

$$\tau = \ln\left\{\frac{hc}{ho}\right\}\left\{\frac{1}{2k_4 k_5 n_o f_o}\right\}^{1/2} \qquad \ldots(24)$$

Thus, for a batch reaction $\tau \alpha \frac{1}{(n_o f_o)^{1/2}}$

Evaluation with $h_c = 10^{-4}$ mol/L., $h_o = 10^{-8}$ mol/L., $k_{4_3} = 1.5 \times 10^4$ L/mol•min and $k_5 = 2 \times 10^3$ L/mol•min gives $\tau = 1.2 \times 10^{-3}$ min = 0.07 s.

Clearly, the reaction should begin almost instantaneously. Saum et al. give no data on induction time. In simple beaker experiments done here, concentrated HCOOH was added to 3 M HNO_3 which had just begun to boil. Induction times were about 45 seconds. This poor prediction of induction time is an indication that equations for additional reactions may be needed early in the denitration process.

4.2 Semi-Batch Experiments

The simulated high level liquid waste of Saum et al. was 6.3 mol/L in HNO_3. They did not do batch experiments with solution at this acidity, but rather semi-batch experiments in which the HCOOH was added slowly at a constant rate to the waste solution. An estimate of the formic acid addition rate of 0.042 mol/L•min was made from the slope of their f vs θ curve at θ = 38 min.

Figures 9 and 10 compare their data with predictions from the two models developed here. Only the formate radical model was used initially, then only the HNO• radical model was used after HCOOH addition stopped because the HNO_3 concentration was ~1 mol/L. The comparison shows that trends are predicted well, although absolute values may be different by up to twofold. While the rate constants and the formic acid addition rate could be adjusted to make the models fit the data better, that was not the objective of this work. The discontinuity in the models' predictions at θ = 38 min is caused by using new initial conditions for the solution at that time since formic acid addition had stopped.

5. CONCLUSIONS

(i) Both the HNO• radical cycle and the HCOO• radical cycle can predict the trends in HNO_3 and HCOOH concentration data in the batch experiments by Saum et al.

(ii) The HNO• radical cycle model predicts the stoichiometry observed by Saum et al. at < 1 mol/L. HNO_3, which is $\frac{df}{dn} = 2$. Similarly, the HCOO• radical model predicts $\frac{df}{dn} = 1.5$ observed for 1-4 mol/L HNO_3. The HCOO• model predicts $\frac{df}{dn} = 1.5$ at n=0 and clearly does not apply at this limiting concentration.

(iii) Rate constants for the HNO• radical cycle model were chosen to give a reasonable fit to the Saum et al. data. However, key rate constants for the HCOO• radical cycle model were estimated from the literature, and the model also gives a reasonable description of the Saum et al. data with these values. However, the HNO• model must be selected as superior for the Saum et al. batch data because it predicts the correct stoichiometry at $[HNO_3] <$ 1 mol/L.

(iv) The models predict different functional dependencies of the induction time upon initial batch reactant concentrations. For the conditions of Saum et al., the induction time is predicted to be < 0.1 s, yet experiments show an induction time of 45 s. Clearly, the models developed here are not useful for predicting induction time.

(v) Both models, used in tandem, predict the trends observed for the semi-batch experiment given by Saum et al.

REFERENCES

1. J.V.L. Longstaff and K. Singer, The Kinetics of Oxidation by Nitrous Acid and Nitric Acid. Part II Oxidation of Formic Acid in Aqueous Nitric Acid. J. Chem. Soc. (London) 2610-17 (1954).

2. T.V. Healy, "The Reaction of Nitric Acid with Formaldehyde and with Formic Acid and its Application to the Removal of Nitric Acid from Mixtures", J. Appl. Chem. 8 553-61 (1958).

3. C.J. Saum, H. Ford, N. Platts, The Denitration of Simulated Fast Reactor Highly Active Liquor Waste, ND-R-658(S), Risley NPDE, 1981 Nov.

4. E.G. Orebaugh, Denitration of Savannah River Plant Waste Streams, DP-1417, 1976 July.

5. H. Nakamura et al., "Effect of Platinum Group Elements on Denitration of High Level Liquid Waste with Formic Acid", J. Nucl. Sci. and Tech. 15 (10) 42-46, (1978).

6. M. Kubota et al., "Effects of Nitrite on Denitration of Nuclear Fuel Reprocessing Waste with Organic Reductions". J. Nucl. Sci and Tech. 16 (6) 426-433, (1979).

7. M. Kelm et al., "Denitration of Aqueous Waste Solutions from Nuclear Fuel Reprocessing", Nucl. Tech. 51 27-32, (Nov. 1980)

8. K. Holze et al., "Aufstellung eines Reactions modells fur die Denitrierung von Abfallstromen aus der Kernbrennstoff-Aufbereitung", Chemie Ingenieur Technik 51 (7) 754-5 (1979).

9. Carver, M.B. et al., "The FORSIM VI Simulation Package for the Automated Solution of Arbitrarily Defined Partial and/or Ordinary Differential Equation Systems", AECL-5821 (1978).

TABLE 1: Equations of Reaction Mechanisms (Orebaugh (4))

HNO_2-Formation Reactions

(1) $2NO_2 + H_2O \rightarrow HNO_2 + HNO_3$

(2) $NO_2 + HNO^* \rightarrow HNO_2 + NO$

(3) $HNO_3 + HCO_2^* \rightarrow HNO_2 + CO_2 + OH^*$

(4) $HNO_3 + HNO^* \rightarrow 2HNO_2$

HNO_2-Destruction Reactions

(5) $HNO_2 + HCO_2H \rightarrow HNO^* + CO_2 + H_2O$

(6) $HNO_2 + HNO_3 \rightarrow 2NO_2 + H_2O$

(7) $HNO_2 + HCO_2H \rightarrow NO + HCO_2^* + H_2O$

(8) $HNO_2 + HCO_2^* \rightarrow NO + CO_2 + H_2O$

HNO^*-Destruction Reactions

(9) $HNO^* + NO \rightarrow N_2O + OH^*$

(10) $HNO^* + HNO^* \rightarrow N_2O + H_2O$

(11) $HNO^* + HNO^* \rightarrow N_2 + 2OH^*$ (H_2O_2)

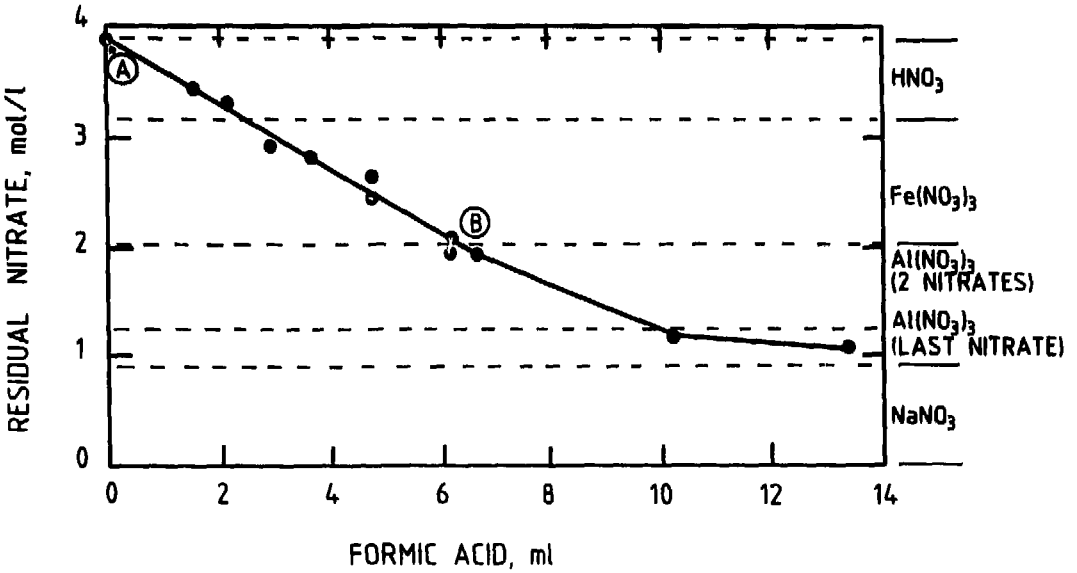

Figure 1: Residual Nitrate versus Formic Acid for SRP Denitration of Simulated Waste - Orebaugh (4)

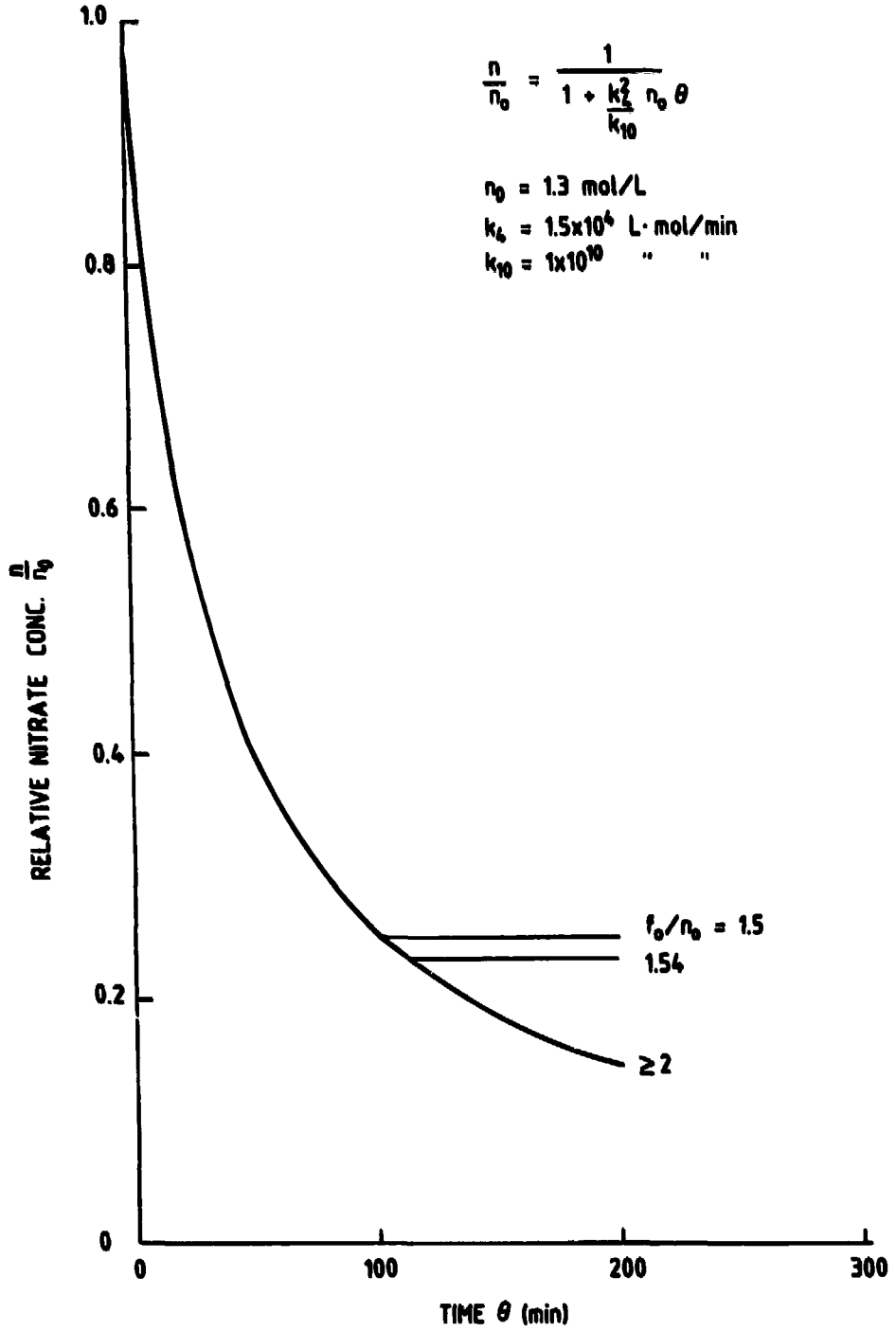

Figure 2: Predicted Nitric Acid Concentration versus Time in a Batch Reaction with Formic Acid: -HNO• radical model

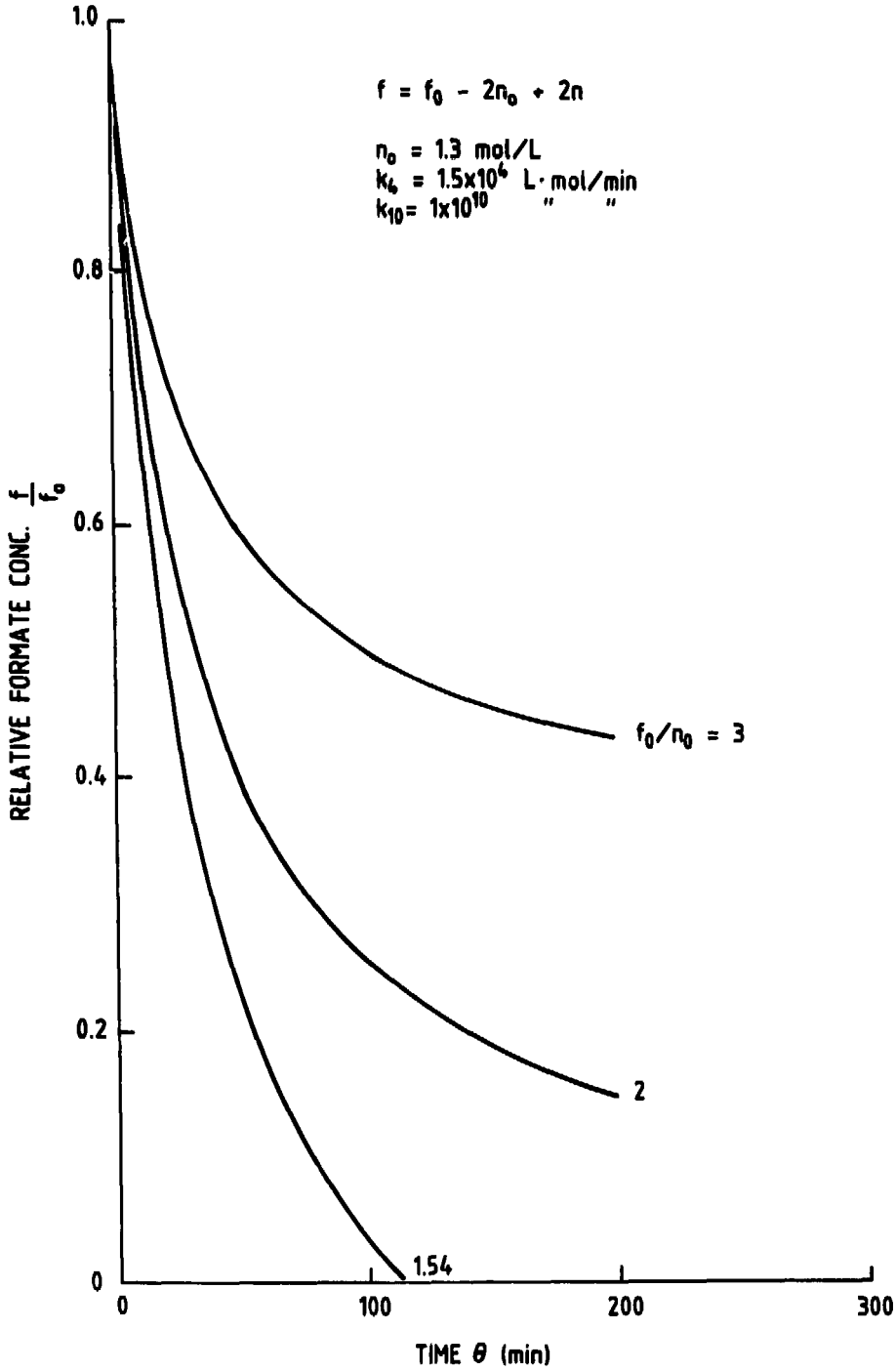

Figure 3: Predicted Formic Acid Concentration versus Time in a Batch Reaction with Nitric Acid: $-HNO^{\bullet}$ Radical Model

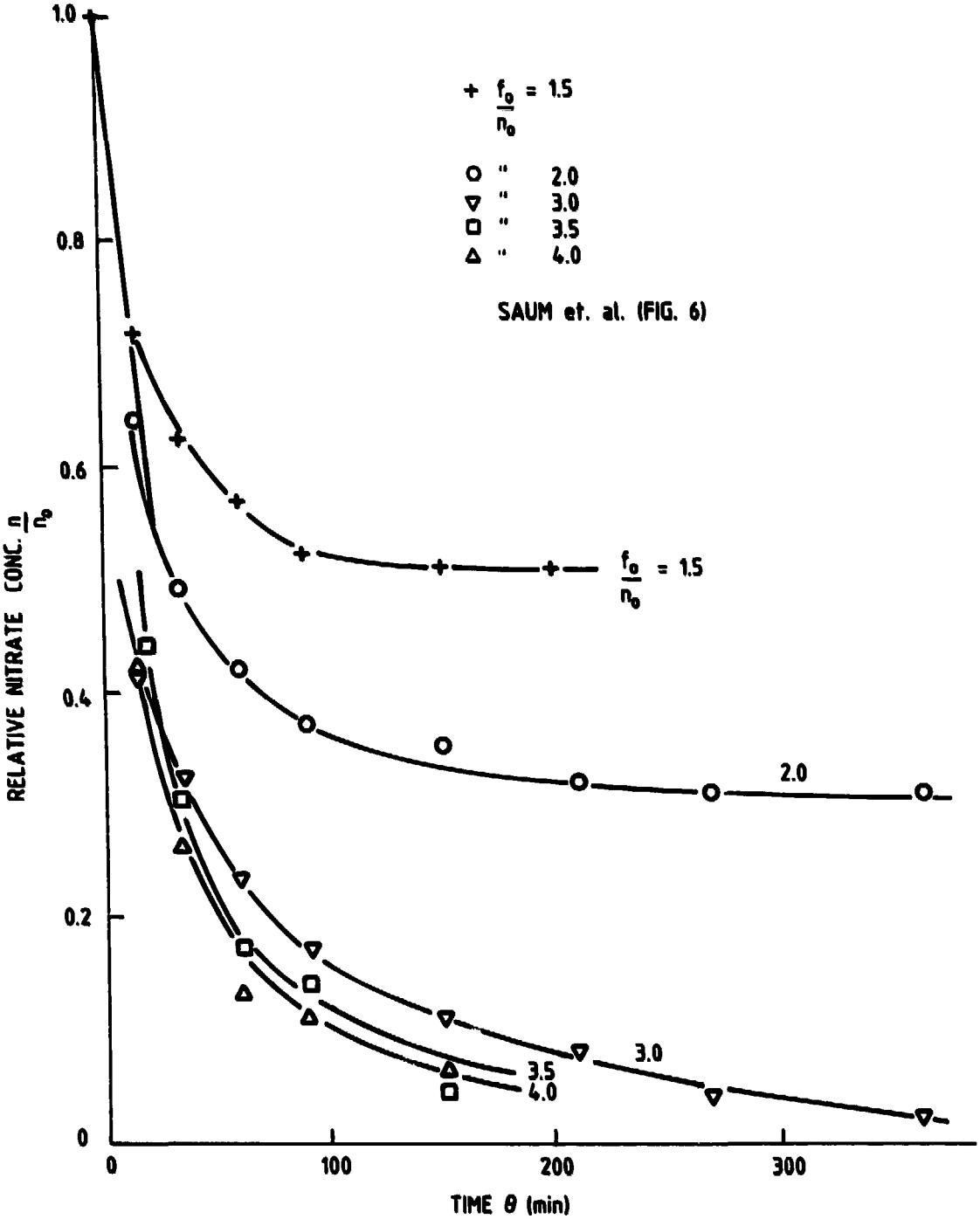

Figure 4: Observed Nitric Acid Concentration versus Time in a Batch Reaction with Formic Acid: Saum et al. data

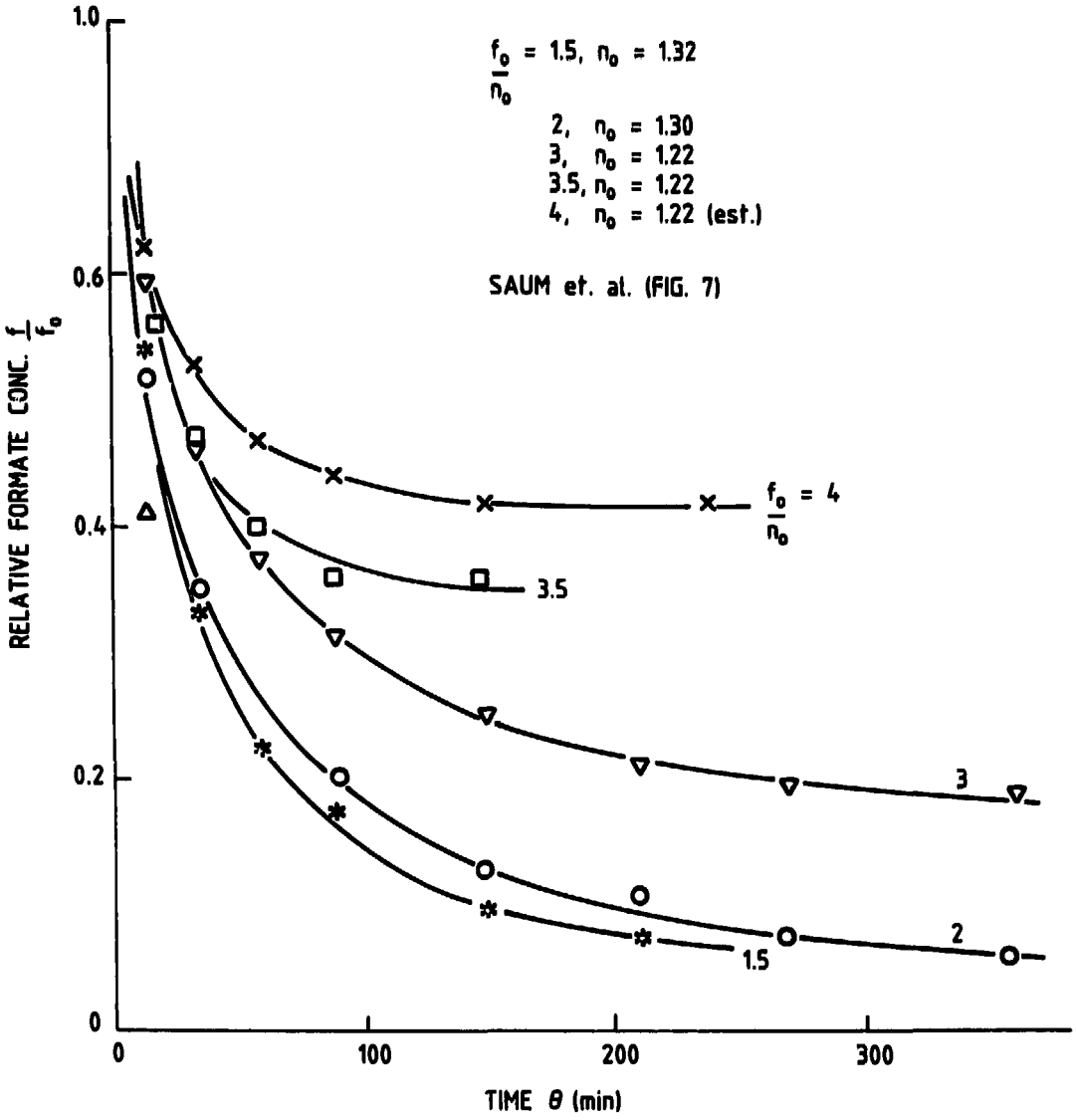

Figure 5: Observed Formic Acid Concentration versus Time in a Batch Reaction with Formic Acid: Saum et al. data

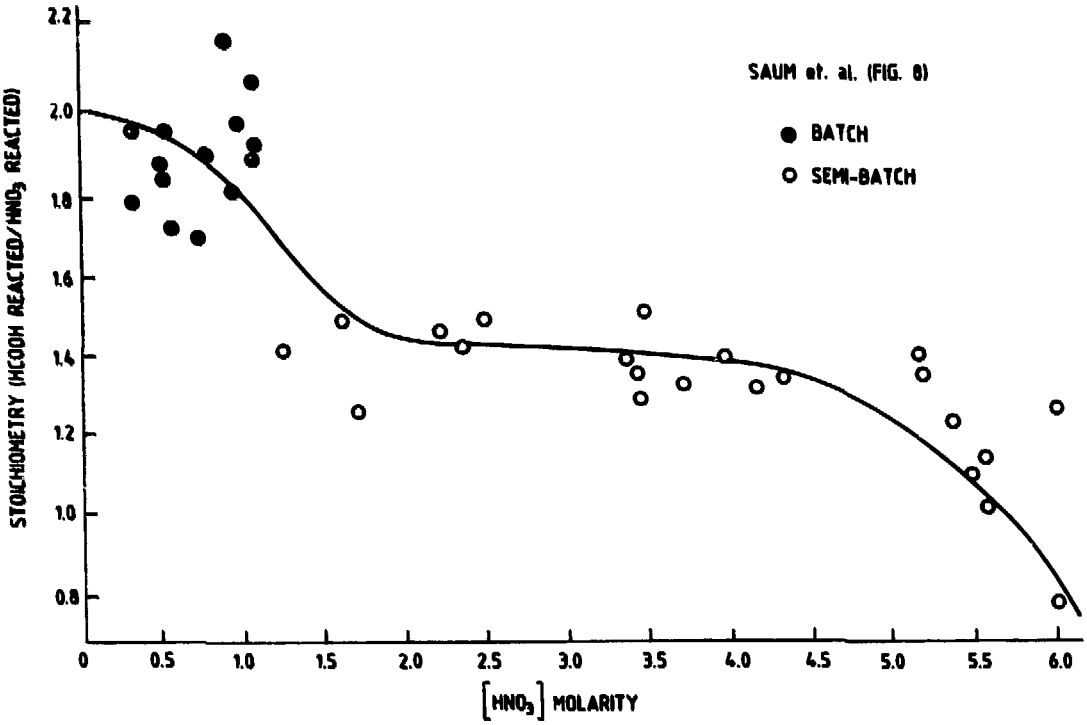

Figure 6: Stoichiometry versus Nitric Acid Concentrations: Saum et al. Data

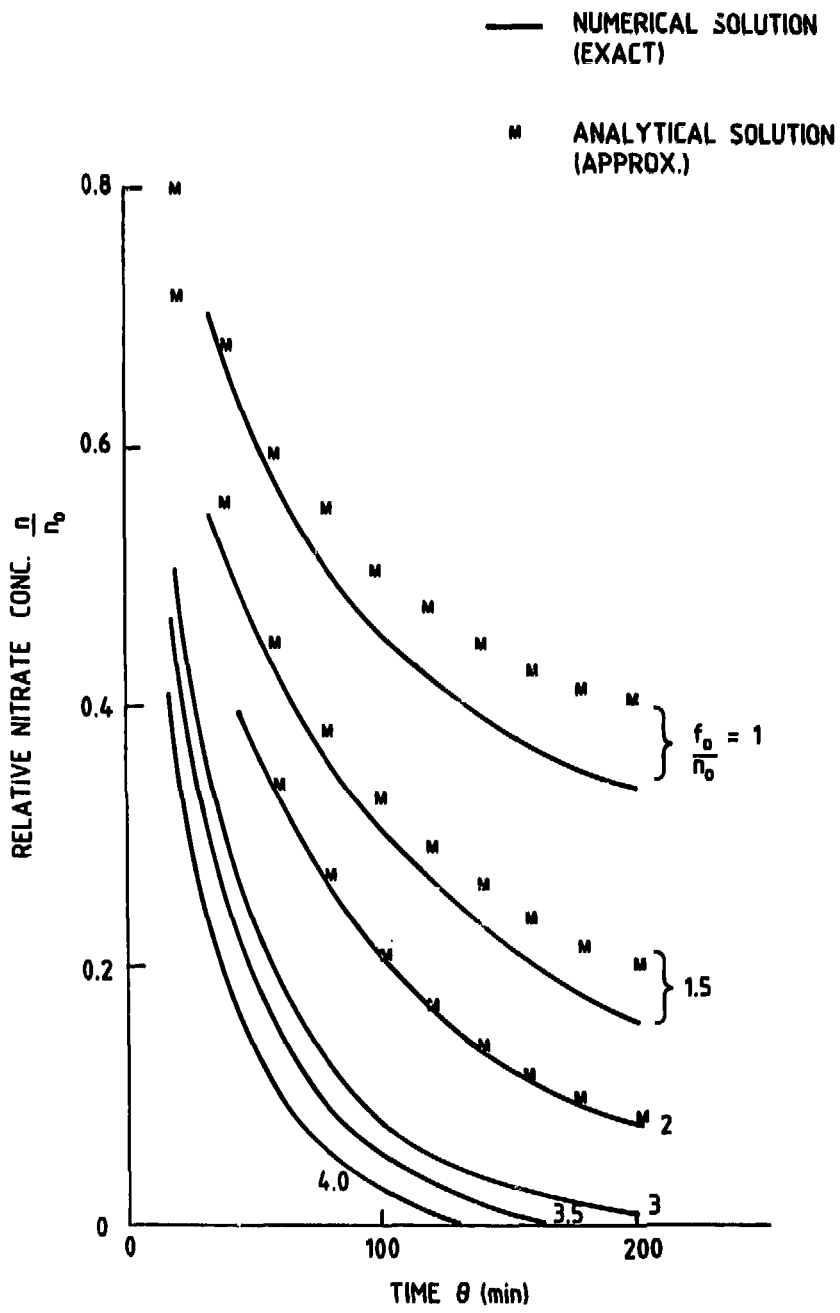

Figure 7: Predicted Nitric Acid Concentration versus Time in a Batch Reaction with Formic Acid: Formate Radical Model.

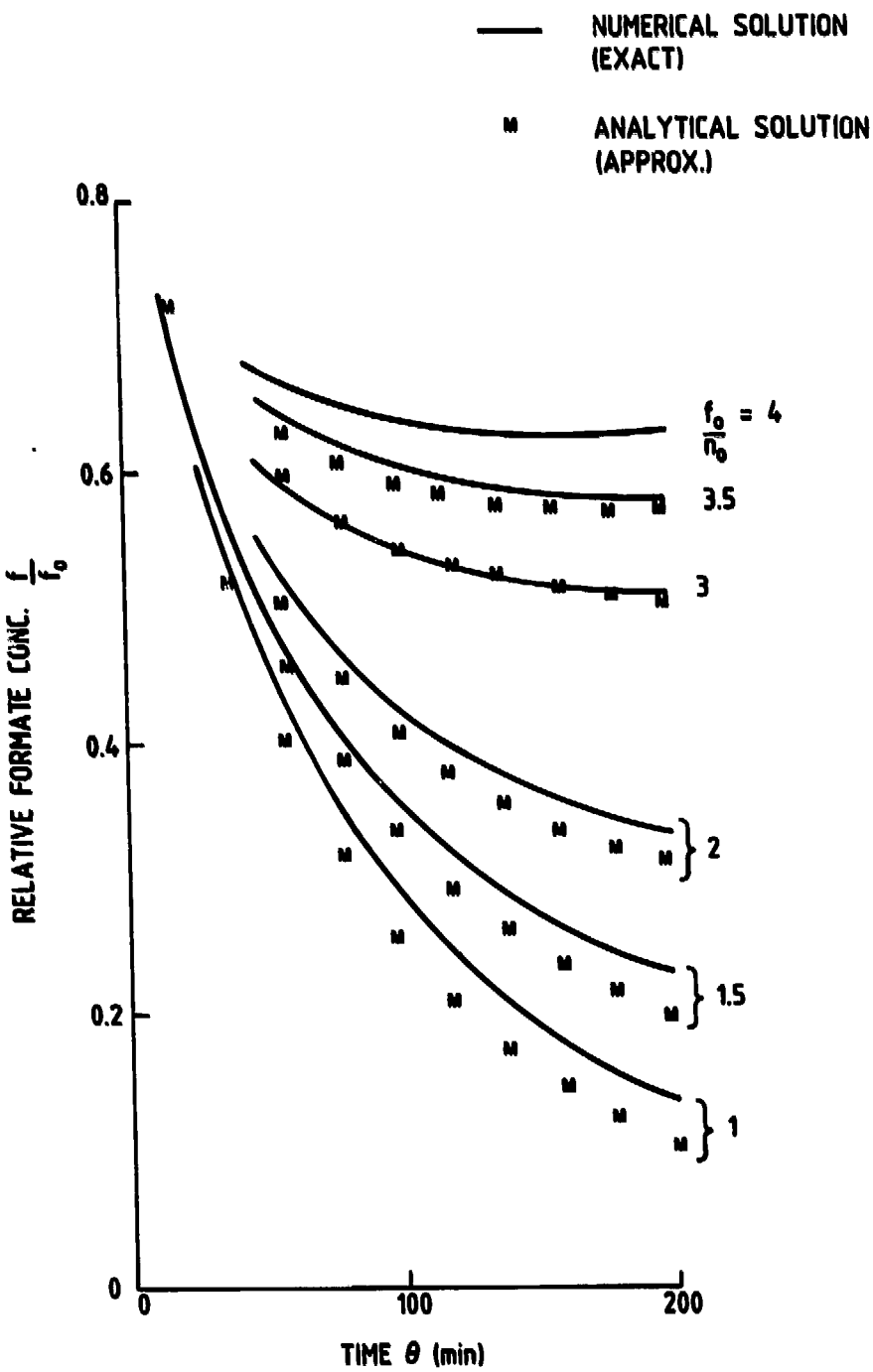

Figure 8: Predicted Formic Acid Concentration versus Time in a Batch Reaction with Nitric Acid: Formate Radical Model.

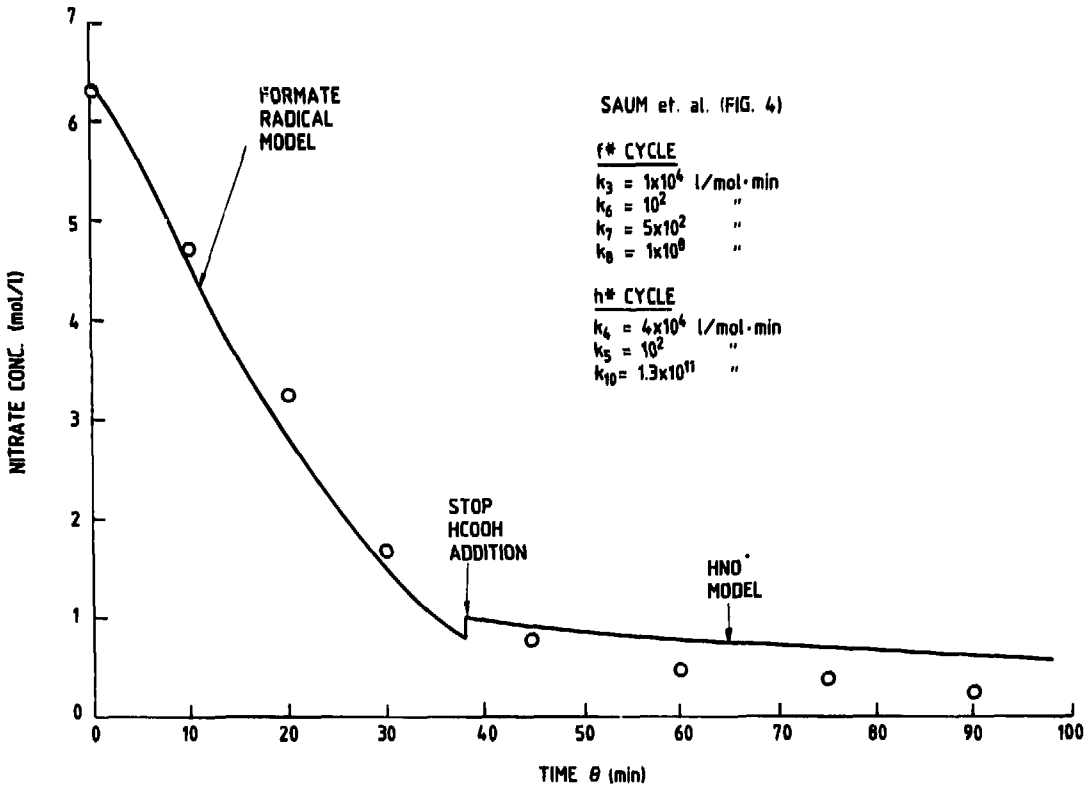

Figure 9: Comparison of Predicted and Observed Nitric Acid Concentration versus Time in a Semi-batch Reaction with Formic Acid: Both Models.

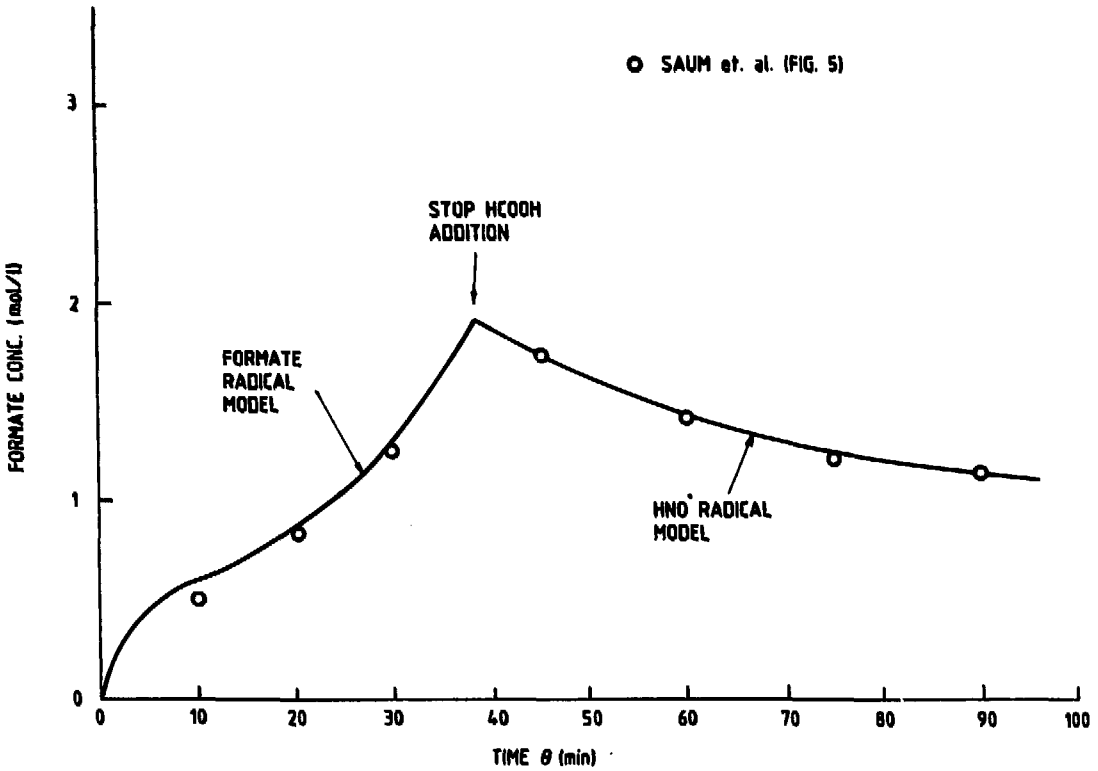

Figure 10: Comparison of Predicted and Observed Formic Acid Concentration versus Time in a Semi-batch Reaction with Nitric Acid: Both Models.

APPENDIX

RATE CONSTANTS FOR POSTULATED REACTIONS

Rate Constants for Postulated Reactions

Saum et al. (3) give the empirical rate expression:

$$\frac{dn}{d\theta} = -K'n^{1.4}f^{1.3} \qquad \ldots(A1)$$

This may be compared with that predicted in equation (12). Ignoring NO_2 production, the model predicts:

$$\frac{dn}{d\theta} = -\frac{k_3 k_7 nf}{k_8}$$

Their data show that $\frac{dn}{d\theta} = -2\times10^{-2}$ mol/min for n=1 mol/L., f=1 mol/L., and 105-110°C. Then $\frac{k_3 k_7}{k_8} = 2 \times 10^{-2}$ L/mol.min

Longstaff et al. (1) studied the kinetics of HCOOH oxidation in HNO_3 and gave an integrated rate expression for the concentration of the nitrous acid intermediate. This is

$$\frac{\ln(h/h_o)}{f} = -K''\theta \qquad \ldots(A2)$$

Equation (14) may be written for simplicity as:

$$\frac{dh}{d\theta} = Cnf - Dhf$$

where NO_2 production has been ignored again. Longstaff et al. kept n and f constant in their experiments so that this equation can be integrated with $h = h_o$, $\theta = 0$ to give:

$$\ln\left\{\frac{Cnf - Dhf}{Cnf - Dh_o f}\right\} = -Df\theta$$

Clearly, for this equation to match Longstaff's, Cnf << Dhf so that

$$\frac{\ln(h/ho)}{f} = -D\theta$$

Longstaff et al. found $K'' = D = 0.8 \times 10^{-2}$ L/mol.min at n = 0.44 mol/L. Then $D = 2k_7 = 8 \times 10^{-3}$ and so $k_7 = 4 \times 10^{-3}$ L/mol.min at 25°C. Holze et al. (6) give E_A = 136 kJ/mol for the rate determining step in denitration, noted by Longstaff et al. as reaction (7), the bimolecular reaction between HNO_2 and HCOOH. Thus, k_7 can be estimated from the Arrhenius expression as:

Arrhenius' Law Applied to k_7

T (K)	k_7 (L/mol•min)
373	247
378	440
383	776

If $k_7 \approx 500$ L/mol.min,

then

$$\frac{k_3}{k_8} = \frac{2 \times 10^{-2}}{500} = 4 \times 10^{-5}$$

The ratio β defined by equation (16) is then:

$$\beta = \frac{k_8}{k_3} = 2.5 \times 10^4$$

The inequality Cnf << Dhf is thus

$$C \ll \frac{Dh}{n}$$

or

$$\frac{k_3}{k_8} \ll \frac{2h}{n}$$

or

$$\frac{1}{\beta} \ll \frac{2h}{n}$$

Longstaff et al. do not give h, but if h is 10^{-4} to 10^{-2} mol/L as found in FORSIM solutions and n ≈ 1 mol/L, then the inequality is satisfied.

ISSN 0067 - 0367

To identify individual documents in the series we have assigned an AECL- number to each.

Please refer to the AECL- number when requesting additional copies of this document

from

Scientific Document Distribution Office
Atomic Energy of Canada Limited
Chalk River, Ontario, Canada
K0J 1J0

Price: A

ISSN 0067 - 0367

Pour identifier les rapports individuels faisant partie de cette série nous avons assigné un numéro AECL- à chacun.

Veuillez faire mention du numéro AECL- si vous demandez d'autres exemplaires de ce rapport

au

Service de Distribution des Documents Officiels
L'Energie Atomique du Canada Limitée
Chalk River, Ontario, Canada
K0J 1J0

Prix: A

192-88